Earthquakes and Structures, *Vol. 7, No. 5 (2014) 735-751*
DOI: http://dx.doi.org/10.12989/eas.2014.7.5.735

Unified equivalent frame method for flat plate slab structures under combined gravity and lateral loads – Part 2: verification

Seung-Ho Choi[1a], Deuck Hang Lee[1b], Jae-Yuel Oh[1c], Kang Su Kim[*1], Jae-Yeon Lee[2d] and Myoungsu Shin[3e]

[1]*Department of Architectural Engineering, University of Seoul, 163 Siripdaero, Dongdaemun-gu, Seoul, 130-743, Korea*
[2]*Division of Architecture, Mokwon University, 88 Doanbuk-ro, Seo-gu, Daejeon, 302-729, Korea*
[3]*School of Urban and Environmental Engineering, UNIST, 50 UNIST-gil, Ulsan, 689-798, Korea*

(Received March 5, 2014, Revised April 30, 2014, Accepted May 6, 2014)

Abstract. In the previous paper, authors proposed the unified equivalent frame method (UEFM) for the lateral behavior analysis of the flat plate structure subjected to the combined gravity and lateral loads, in which the rotations of torsional members were distributed to the equivalent column and the equivalent slab according to the relative ratio of gravity and lateral loads. In this paper, the lateral behavior of the multi-span flat plate structures under various levels of combined gravity and lateral loads were analyzed by the proposed UEFM, which were compared with test results as well as those estimated by existing models. In addition, to consider the stiffness degradation of the flat plate system after cracking, the stiffness reduction factors for torsional members were derived from the test results of the interior and exterior slab-column connection specimens, based on which the simplified nonlinear push-over analysis method for flat plate structures was proposed. The simplified nonlinear analysis method provided good agreements with test results and is considered to be very useful for the practical design of the flat plate structures under the combined gravity and lateral loads.

Keywords: flat plate; lateral load; gravity load; equivalent frame method; torsion; stiffness degradation, push-over analysis

1. Introduction

In the previous paper by authors, (Kim *et al*. 2014) the existing methods (Corely *et al*. 1961, Corely and Jirsa 1970, Vanderbilt 1981, Vanderbilt and Corely 1983, Hwang and Moehle 2000, Murray *et al*. 2003) for the lateral behavior analysis of the reinforced concrete flat plate structures were thoroughly reviewed, and their shortcomings were discussed in detail. To overcome the

*Corresponding author, Professor, E-mail: kangkim@uos.ac.kr
a Ph.D. Student, E-mail: ssarmilmil@hanmail.net
b Ph.D. Candidate, E-mail: dklee@uos.ac.kr
c Ph.D. Candidate, E-mail: hahappyppy@naver.com
d Professor, E-mail: jylee@mokwon.ac.kr
e Associate Professor, E-mail: msshin@unist.ac.kr

 ISSN: 2092-7614 (Print), 2092-7622 (Online)

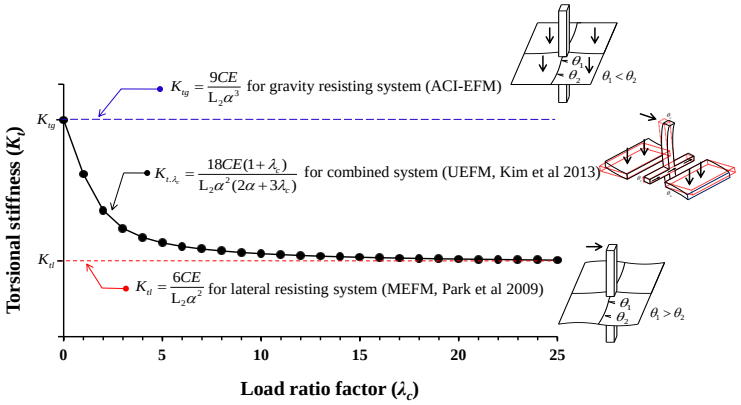

Fig. 1 Torsional stiffness change of transverse member according to load ratio factor

limitations of existing models, the unified equivalent frame method (UEFM) was proposed in the previous study, which can be applicable to the lateral behavior analysis of the flat plate structures under the combined gravity and lateral loads. In the UEFM, the stiffness of a torsional member in the equivalent frame was derived, as follows

$$K_{t,\lambda_c} = \frac{18CE_c\left(1+\lambda_c\right)}{L_2\alpha^2\left(2\alpha+3\lambda_c\right)} \tag{1}$$

where C is the torsional constant, E_c is the modulus of elasticity of concrete, λ_c is the load combination factor, α is $1-c_2/L_2$, L_2 is the slab width perpendicular to the design strip, and c_2 is the column width in the L_2 direction. As shown in Fig. 1, the torsional stiffness presented in Eq. (1) ranges from that of gravity system to that of lateral resisting system.

In this paper, the lateral behavior of multi-span flat plate structures under various levels of combined gravity and later loads is analyzed by the UEFM, which is also compared with those estimated by existing models and test results for its verification. On the other hand, since the UEFM was developed as an analysis method for the flat plate system within elastic range, it was not suitable for inelastic behavior analysis. Thus, in order to consider the lateral stiffness degradation of the flat plate system after cracking, the torsional stiffness reduction factors have been also formulated for exterior and interior slab-column connections, which can account for the effect of gravity loads and the geometric characteristics of columns and slabs. The nonlinear analysis model for the flat plate system under the combined loads, which has been extended from the UEFM, has been also verified by comparing to test results.

2. Evaluation of unified equivalent

Fig. 2(a) shows the dimensional properties of test specimens performed by Hwang and Moehle (1993) at the University of California, Berkeley (UCB), and Fig. 2(b) and (c) show the comparisons of their test results and the analysis results by the UEFM and other existing models. In this plot, the analysis results of equivalent frame method (EFM) were obtained from the

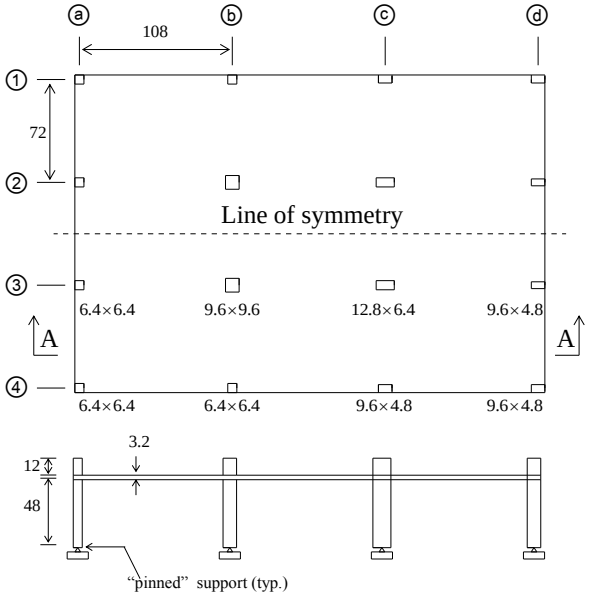

SECTION A-A

(All unit are in inches, 1 in = 25.4mm)

(a) Dimension details of UCB test specimen (Hwang and Moehle 2003)

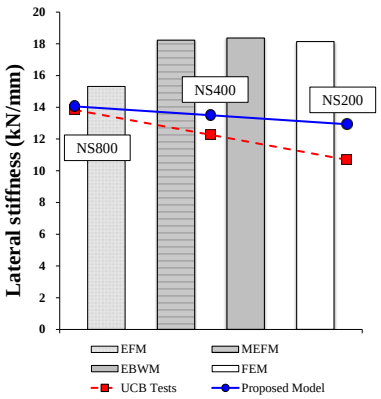

(b) NS direction

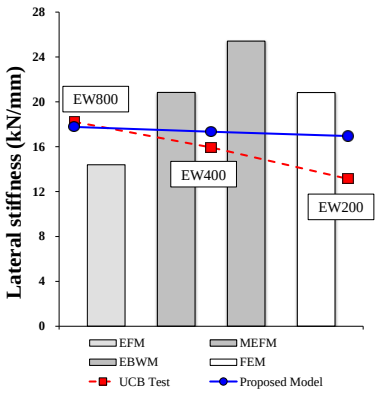

(c) EW direction

Fig. 2 Comparison of test and analysis results

analysis method presented in ACI 318-11 (2011), and the analysis results of modified equivalent frame method (MEFM) and effective beam width method (EBWM) were estimated by the approaches presented by Park *et al*. (2009) and Banchik (1983), respectively. The FEM analysis results were those reported by Hwang and Moehle (2000). The labels of NS800, NS400 and NS200 stand for the loading stage at the target drift ratio of 1/800, 1/400 and 1/200, in the NS direction, respectively, and similarly, EW800, EW400 and EW200 are the same loading stages in

the EW direction. Note that the gravity load was 5650 Pa (N/m^2) including the self-weight of the specimen, and the columns had all different flexural stiffness. Other detailed information on the test specimen and the experimental program can be found in Hwang and Moehle (1993, 2000). It should be also noted that any stiffness degradation due to cracking or yielding of reinforcement was not considered in all analysis. Among the analysis results of existing methods in the NS direction as shown in Fig. 2(b), ACI-EFM provided the closest lateral stiffness to the test results at the 1/800 drift ratio, which is considered to be because the effect of the lateral load was minimal at the low drift level, like 1/800, while MEFM, EBWM and FEM showed relatively larger lateral stiffness than the observed values. Fig. 2(c) showed the test and analysis results in the EW direction, in which the effective depths of all columns were different with each other. While the lateral stiffness estimated by MEFM and FEM provided reasonable estimations of the test results, ACI-EFM showed the lowest lateral stiffness, and EBWM provided much larger stiffness than other results. The overestimation of EBWM seems to be due to the irregular geometric characteristics of columns provided in the EW direction, as it was basically derived from two-way slabs having regular column configurations. It is appeared that the existing methods provided relatively better estimations on the lateral stiffness of the specimens when the drift ratio was low, whereas the proposed model well estimated the lateral stiffness changes of the flat plate system for various levels of drift ratios in elastic range without any stiffness reduction factor in both NS and EW directions. This is because, as the lateral drift ratio increases, as shown in Fig. 1, the ratio of lateral load to the gravity load (λ_c) increases in the proposed model, which decreases the stiffness of the torsional member and, in turn, reduces the stiffness of both equivalent columns and equivalent slabs. This is good in that the proposed UEFM can reasonably evaluate the lateral stiffness behavior without considering the stiffness degradation. However, in the lateral drift ratio over 1/400, multiple flexural cracks were observed in the slabs of specimen, leading to more severe degradation of lateral stiffness. Therefore, the stiffness degradation should be considered for more accurate evaluation of lateral response of flat plate systems under relatively large drift levels. (Hwang and Moehle 1993)

3. Simplified nonlinear push-over analysis method

3.1 Stiffness degradation of flat plate structure

ACI 318-11 (2011) specifies the reduction of the effective beam width from 1/2 to 1/4 that accounts for the effect of cracking on the stiffness of non-prestressed members. Also, it is stated that, if the stiffness values are not obtained by the comprehensive analysis taking into account the effects of cracking and reinforcement on the member stiffness, the effective moment of inertia of slab members may be computed as a fully-cracked section, and, alternatively, the effective moment of inertia can be determined based on test results of full-sized specimens. (Vanderbilt and Corely 1983) Thus, the current design standard (ACI 318-11) allows the designer to use the stiffness based on any approaches as long as it satisfies the equilibrium and compatibility conditions, or it is verified by test data. The flexural stiffness reduction factor recommended in the commentary of ACI 318-11(2011) is based on the lower bound value of 1/3 proposed by Vanderbilt and Corely (1983), Moehle and Diebold (1985), and Pan and Moehle (1988). Although it is simple and easy to implement, it is expected that, as the stiffness reduction factor is constant,

it cannot help providing a limited accuracy of estimating the nonlinear lateral response of the two-way flat plate system. It is, of course, also difficult to reflect the effect of combined gravity and lateral loads. Therefore, based on the test results by Hwang and Moehle (1993), Grossman (1997) proposed the effective beam width model considering the stiffness degradation according to the level of lateral drift. Luo and Durrani (1995a, b) also proposed the slab stiffness reduction factor (χ) as the function of the gravity-shear ratio (V_g/V_c). As pointed out by Han *et al*. (2009), however, their stiffness reduction factor requires the calculation of the amount of reinforcement provided in the slab member, which is very difficult to estimate in the beginning stage of design. Recently, based on various existing test results of flat plate slab-column members, Han *et al*. (2009) reported that the amount of reinforcement in slab members did not have a significant effect on the stiffness degradation of flat plate systems. They also proposed the empirical stiffness reduction factor for the EBWM based on the nonlinear regression analysis of test results, which considered the ratio of the applied moment to the cracking moment of the slab (M_a / M_{cr}) as the key factor. The stiffness reduction factor proposed by Han *et al*. (2009) considered the effect of gravity load in a very simple way, and it also provided a reasonable accuracy for estimating the nonlinear behavior of the flat plate interior and exterior connection specimens. As aforementioned, however, since the stiffness degradation of a flat plate system under combined gravity and lateral loads is caused by the stiffness degradation of columns as well as slab members, the stiffness degradation in slabs, columns, and slab-column connections should be considered simultaneously. (Moehle and Diebold 1985, Robertson 1990, Du 1993, Hwang and Moehle 1993) There are advanced nonlinear analysis methods, (Prakash 1993, McKenna *et al*. 2000, Carr 2005, Coronelli 2010, Elnashai *et al*. 2010, Carvalho *et al*. 2013, Karimiyan *et al*. 2013, Lee *et al*. 2013, Coronelli and Corti 2014) some of which provide a good level of accuracy. They are, however, yet inefficient because they require considerable analytic cost, and the reliability of the analysis results still largely depends on the experts' experience. (Cano and Klingner 1987, Park *et al*. 2009, Ghobarah 2001) This is why Han *et al*. (2009) proposed the stiffness reduction factor to make it simple.

This study proposed an approach that can simply reflect the stiffness degradation induced in slabs, columns, and slab-column connections by reducing the torsional member stiffness. Such a point of view on the stiffness degradation of flat plate structure can also be found in the study of Hwang and Moehle (2000). They presented that reducing the stiffness of the torsional member is a better approach than other approaches, because, for example, the stiffness degradation of slabs only cannot lead to consider the redistribution of the bending moment developed in the end region of the slabs, due to the accumulated damage in the slab-column connection, toward the central part of slab.

3.2 Stiffness degradation due to gravity loads

The actual flexural stiffness of a flat plate slab under gravity loads (K_I) is generally smaller than the elastic flexural stiffness (K_0) calculated by the gross section properties of the slab. (Schwaighofer and Collins 1977, Hwang and Moehle 2000, Choi and Park 2003) Fig. 3 shows the numerical analysis results performed by Choi and Park (2003), based on which they presented the initial stiffness degradation ratio of the slab (K_I / K_o) according to the gravity-shear ratio (V_g/V_c), as follows:

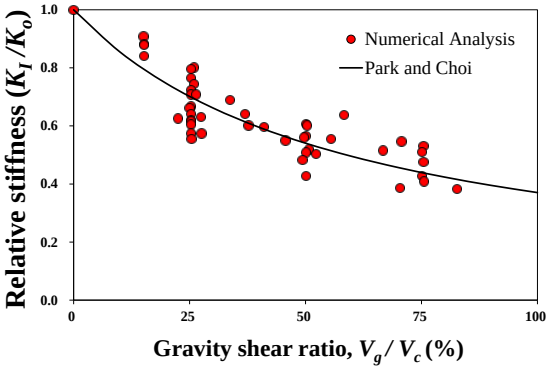

Fig. 3 Initial stiffness degradation in slab due to gravity shear (Choi and Park 2003)

$$\eta_g = \frac{K_I}{K_0} = \frac{1}{1.7(V_g/V_c)+1} \tag{2}$$

where, V_g is the external gravity shear force, and V_c is the punching shear strength.

Considering the initial stiffness degradation of the slab due to the gravity-shear ratio (V_g/V_c), the effective slab stiffness ($K_{s,eff}$) can be expressed, as follows:

$$K_{s,eff} = \eta_g K_s \tag{3}$$

where K_s is the flexural stiffness of the slab. Then, the flexibility of the equivalent column (K_{ec}) and equivalent slab (K_{es}) can be computed, respectively, as follows:

$$\frac{1}{K_{ec}} = \frac{\sum K_c}{\sum K_c + \sum K_{s,eff}} \frac{1}{K_{t,\lambda_c}} + \frac{1}{\sum K_c} \tag{4}$$

$$\frac{1}{K_{es}} = \frac{\sum K_{s,eff}}{\sum K_c + \sum K_{s,eff}} \frac{1}{K_{t,\lambda_c}} + \frac{1}{\sum K_{s,eff}} \tag{5}$$

where K_c is the flexural stiffness of the column.

3.3 Stiffness degradation due to unbalanced moment

When the flat plate structure is subjected to lateral load, unbalanced moment is developed at the slab-column connection, which increases the torsional moment induced in the transverse member, i.e., the torsional member. In order to model the stiffness degradation in a simply way, this study adopted an assumption that all the stiffness degradation of the flat plate system can be expressed

consistently by the torsional member stiffness, except for the initial stiffness degradation of the slab induced by the gravity-shear effect expressed in Eq. (2). Then, the stiffness degradation in slabs, columns, and slab-column connections can be considered by introducing a well-calibrated stiffness reduction factor of the torsional member (η_l) in a simple manner.

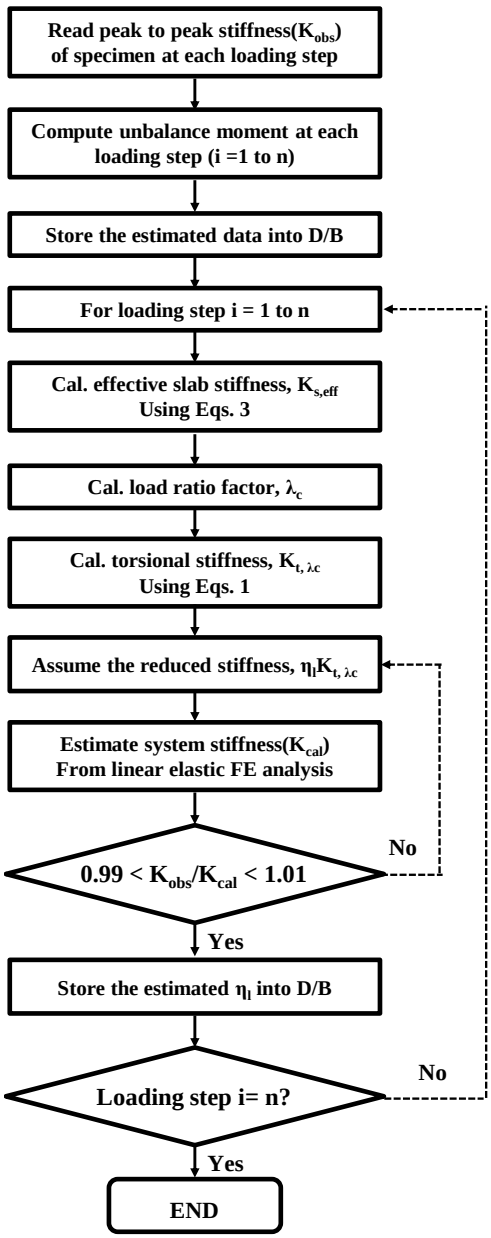

Fig. 4 Flow chart for estimation of torsional stiffness reduction factor (η_l)

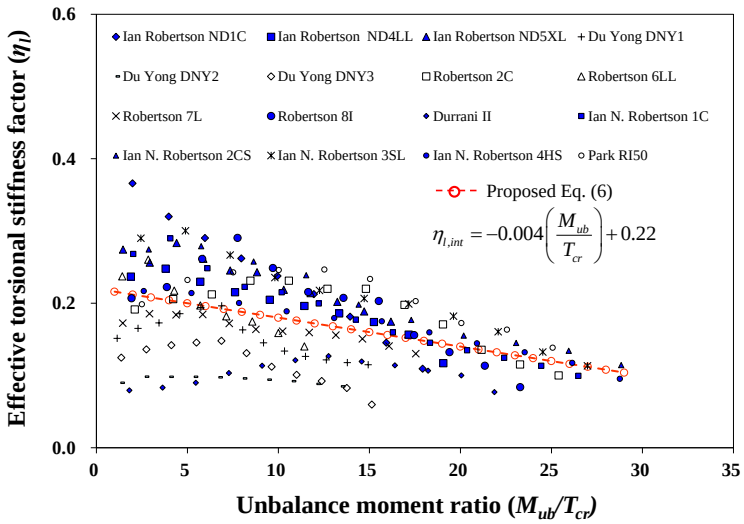

Fig. 5 Relation between stiffness degradation of torsional member and unbalance moment (interior specimens)

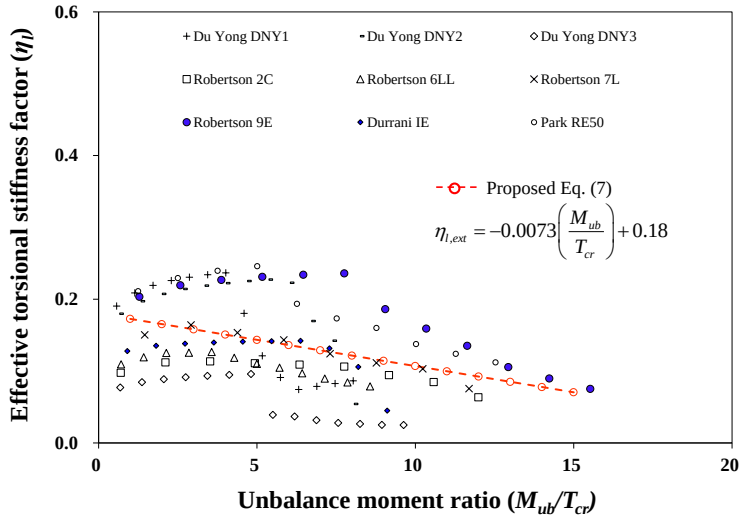

Fig. 6 Relation between stiffness degradation of torsional member and unbalance moment (exterior specimens)

The stiffness reduction factor of the torsional member (η_l) can be determined based on the correlation between the stiffness changes collected from test results and the unbalanced moments. For this purpose, sixteen interior and nine exterior slab-column connection specimens were collected from literature. (Robertson 1990, Du 1993, Luo *et al*. 1994, Robertson *et al*. 2002, Robertson and Johnson 2006, Han *et al*. 2009) Among sixteen test results of the interior connection specimens, ten were obtained from the interior slab-column sub-assembly tests, while

the rest were from the measured responses of interior connections in two-span frame specimens. Among nine test results of the exterior connection specimens, three were obtained from the exterior slab-column sub-assembly tests, while the rest were from the measured responses of exterior connections in two-span frame specimens. The dimensional details, gravity load levels, and material properties of interior and exterior connection specimens were shown in Tables 1 and 2 in detail, respectively.

Fig. 4 shows the calculation procedure of the proposed stiffness reduction factor for the torsional member. By substituting the torsional stiffness (K_{t,λ_c}) estimated by Eq. (1) and the effective slab stiffness ($K_{s,eff}$) by Eq. (2) into Eqs. (4) and (5), the stiffness of the equivalent slab and the equivalent column (K_{es} and K_{ec}) can be determined, respectively, and the values of K_{es} and K_{ec} were used to calculate the stiffness of the system, i.e., the ratio of the lateral force to the corresponding lateral drift ratio (K_{cal}). The ratio between the estimated system stiffness (K_{cal}) and the observed stiffness of the specimen at each loading stage (K_{obs}) is defined as the stiffness reduction factor of the torsional member (η_l). The stiffness reduction factors of the torsional member in the interior and exterior connections, estimated by the aforementioned calculation procedure, are shown in Figs. 5 and 6, respectively. Based on the regression analysis of the calculated torsional stiffness, the stiffness reduction factor of the torsional member in the interior and exterior connections ($\eta_{l,\text{int}}$ and $\eta_{l,\text{ext}}$) was determined, as follows

$$\eta_{l,\text{int}} = -0.004\left(\frac{M_{ub}}{T_{cr}}\right) + 0.22 \tag{6}$$

$$\eta_{l,\text{ext}} = -0.0073\left(\frac{M_{ub}}{T_{cr}}\right) + 0.18 \tag{7}$$

where, the cracking strength of the torsional member (T_{cr}) was adopted from ACI 318-11 (2011) as $1/3\sqrt{f_c'}A_{cp}^{\ 2}/p_{cp}$, and $f_c^{'}$ is the compressive strength of concrete, A_{cp} is the sectional area of shear flow zone, and p_{cp} is the perimeter of shear flow zone. To simplify the computation of torsional cracking strength, A_{cp} and p_{cp} were defined as $c_1 t$ and $2(c_1 + t)$, respectively, where c_1 is the column width in loading direction, and t is the slab thickness. Then, the flexibility of the equivalent column and the equivalent slab considering the stiffness degradation induced by gravity and lateral loads can be expressed, respectively, as follows

$$\frac{1}{K_{ec}} = \theta_{t,gravity} + \theta_c = \frac{\sum K_c}{\sum K_c + \sum K_{s,eff}} \frac{1}{\eta_l K_{t,\lambda_c}} + \frac{1}{\sum K_c} \tag{8}$$

$$\frac{1}{K_{es}} = \theta_{t,lateral} + \theta_c = \frac{\sum K_{s,eff}}{\sum K_c + \sum K_{s,eff}} \frac{1}{\eta_l K_{t,\lambda_c}} + \frac{1}{\sum K_{s,eff}} \tag{9}$$

Table 1 Details of interior connection specimens

Researchers	Label	Dimensions (mm)								Gravity load		f_c' (MPa)
		L_1	L_2	t	c_1	c_2	h_1	h_2	d_{ave}	V_g (kN)	V_g/V_c	
Robertson and Johnson (2006)	ND1C	3048	2743	114	254	254	686	686	100	60.8	0.237	29.6
	ND4LL	3048	2743	114	254	254	686	686	100	93.4	0.348	32.3
	ND5XL	3048	2743	114	254	254	686	686	100	104.8	0.452	24.1
Du(1993)	DNY1	2900	1980	114	254	254	648	648	102	59.34	0.206	35.3
	DNY2	2900	1980	114	254	254	648	648	102	68.85	0.281	25.7
	DNY3	2900	1980	114	254	254	648	648	102	59.34	0.247	24.6
Robertson (1990)	2C	2900	1980	114	254	254	770	770	92	52.93	0.217	33.0
	6LL	2900	1980	114	254	254	770	770	92	120.99	0.502	32.2
	7L	2900	1980	114	254	254	770	770	92	90.74	0.386	30.8
	8I	2900	1980	114	254	254	770	770	92	52.93	0.199	39.3
Luo *et al.* (1994)	II	2900	1980	114	254	254	757.5	817.5	102	15.71	0.071	20.7
Robertson *et al.*(2002)	1C	3000	2750	115	250	250	762.5	762.5	95	65.0	0.250	35.4
	2CS	3000	2750	115	250	250	762.5	762.5	95	66.12	0.270	31.4
	3SL	3000	2750	115	250	250	762.5	762.5	95	66.21	0.230	43.4
	4HS	3000	2750	115	250	250	762.5	762.5	95	64.82	0.240	38.2
Han *et al.* (2009)	RI-50	3400	3600	130	300	300	1050	1050	110	122.6	0.359	32.3

where, L_1 : length of slab in design direction, L_2 : length of slab in perpendicular to design direction, t : slab thickness, c_1 : column width in design direction, c_2 :column width in perpendicular to design direction, h_1 :height of upper column, h_2 : height of bottom column, d_{ave} :average effective depth of slab, V_g : gravity shear force, V_g / V_c : gravity shear ratio, f_c' : compressive strength of concrete

Table 2 Details of exterior connection specimens

Researchers	Label	Dimensions (mm)								Gravity load		f_c' (MPa)
		L_1	L_2	t	c_1	c_2	h_1	h_2	d_{ave}	V_g (kN)	V_g/V_c	
Du(1993)	DNY1	1450	1980	114	254	254	648	648	102	31.63	0.162	35.3
	DNY2	1450	1980	114	254	254	648	648	102	36.75	0.221	25.7
	DNY3	1450	1980	114	254	254	648	648	102	31.63	0.194	24.6
Robertson (1990)	2C	1450	1980	114	254	254	770	770	92	31.14	0.187	33
	6LL	1450	1980	114	254	254	770	770	92	76.07	0.462	32.2
	7L	1450	1980	114	254	254	770	770	92	52.49	0.326	30.8
	9E	1450	1980	114	254	254	770	770	92	31.14	0.171	39.3
Luo *et al.* (1994)	IE	1450	1980	114	254	254	757.5	817.5	102	8.13	0.054	20.7
Han *et al.* (2009)	RE-50	1700	3600	130	300	300	1050	1050	110	86.8	0.372	32.3

4. Verification of simplified push-over analysis method

Shown in Figs. 7(a) and 7(b) are the comparisons between the test results of the interior and exterior connections and those estimated by the UEFM with the proposed stiffness reduction factors. The proposed model estimated the overall lateral behavior of the interior and exterior connections very closely for most cases. However, it overestimated some of test results, in which stiffness degradation at the initial loading stage or at a certain lateral load level was significantly larger than expected due to the excessive slab cracking, steel yielding, concrete crushing, weak-column effect, and accumulated cyclic damages. Since the inter-relations between these influential factors are still unclear and complicated to be completely considered in the analysis model, it is yet difficult to predict the lateral behavior of all of specimens perfectly. However, considering the simplicity of the proposed analysis method compared to other nonlinear analysis approaches, the analysis results is considered to be good enough for practical purpose. It is also worth to note that the effect of the gravity-shear ratio was well captured by the proposed approach. Furthermore, the accuracy of the analysis can be enhanced, once the improved criteria for the determination of deformation capacity of flat plate structures are developed afterward.

For the verification of the UEFM with the proposed stiffness reduction factor in the system level, the test results of multi-span flat plate structures performed by Robertson (1990, 1997) were compared to the analysis results estimated by the proposed UEFM with stiffness reduction factor, as shown in Fig. 8. The key parameter of their test programs was the gravity-shear ratio (V_g/V_c), and the V_g/V_c ratios of the specimen 2C were 0.217 and 0.187 for the interior and exterior connection, respectively, while the specimen 7L were 0.386 and 0.326, and the specimen 6LL were 0.502 and 0.462, respectively. As shown in Fig. 8(a), the span length in all specimens was identical to 2,900 mm, and the compressive strength of concrete was 33.0 MPa for the specimen 2C, 32.2 MPa for the specimen 6LL and 30.8 MPa for the specimen 7L. All specimens were fabricated in one-half scale of the actual reference building, and the columns were 254 mm x 254 mm squared section. It is noted that, among the seven specimens reported by Robertson (1990 and 1997), the specimen 1C whose testing was incompletely terminated due to an unexpected blackout, the specimen 3SE with the edge beam, and the specimen 5SO with the slab extended outside the exterior connection were excluded from the analysis in this study. Also, the specimen 4S with shear reinforcement was excluded from the discussion due to the lack of information on the details of shear reinforcement in the reference. As shown in Figs. 8(b) and (d), the lateral analysis was terminated at the maximum allowable drift ratio ($DR_{\max}$) of the flat plate system without shear reinforcement as specified in ACI 318-11 (2011), which is expressed, as follows

$$DR_{\max} = 0.035 - 0.05\left(V_g / \phi V_c\right) \tag{10}$$

where the strength reduction factor (ϕ) was set to 1.0. The proposed model showed a good estimation on the overall nonlinear lateral responses of not only the specimen 2C with the lowest gravity-shear ratio, but also the specimens 7L and 6LL with relatively large gravity-shear ratios. These results imply that it is very effective to express the stiffness degradation of the flat plate systems under lateral loads as the stiffness reduction of the torsional member. Also, it is appeared that Eq. (10), presented in ACI 318-11 (2011), can evaluate the deformation capacity of flat plate systems at the maximum load in a reasonable accuracy according to the gravity-shear ratio. In order to estimate post-peak responses of flat-plate structures, however, a more advanced evaluation method on the deformation capacity is yet required.

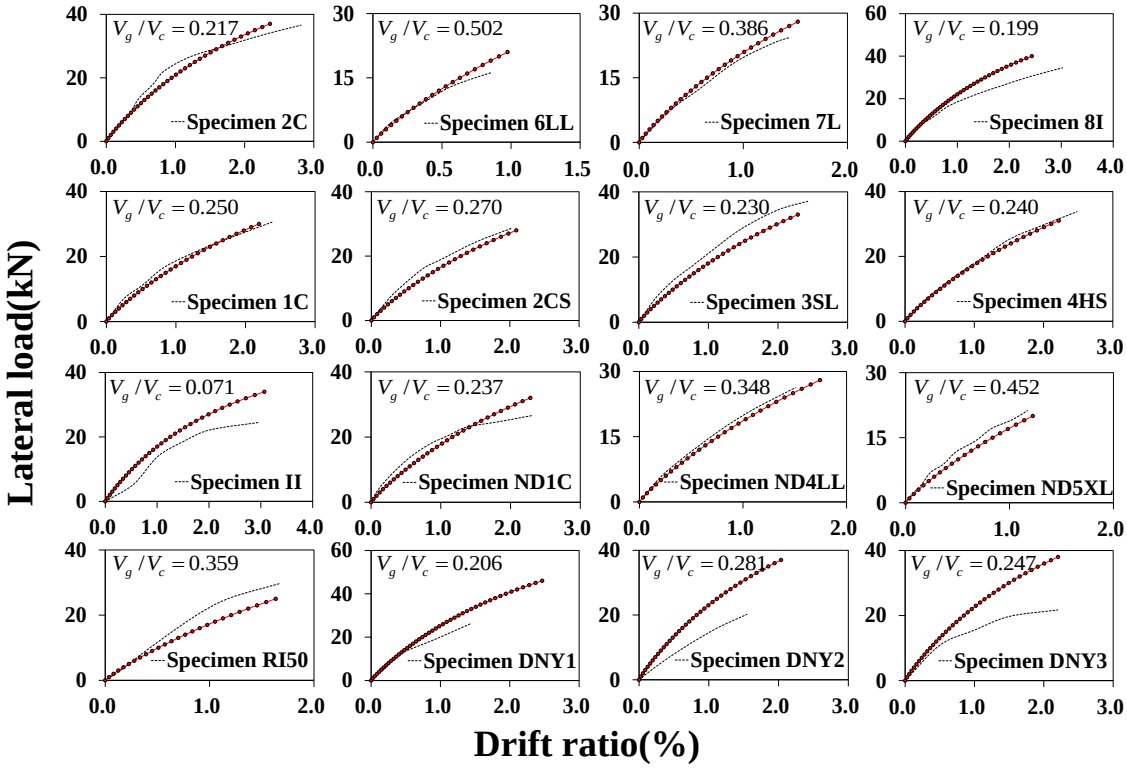

(a) Interior slab-column connections

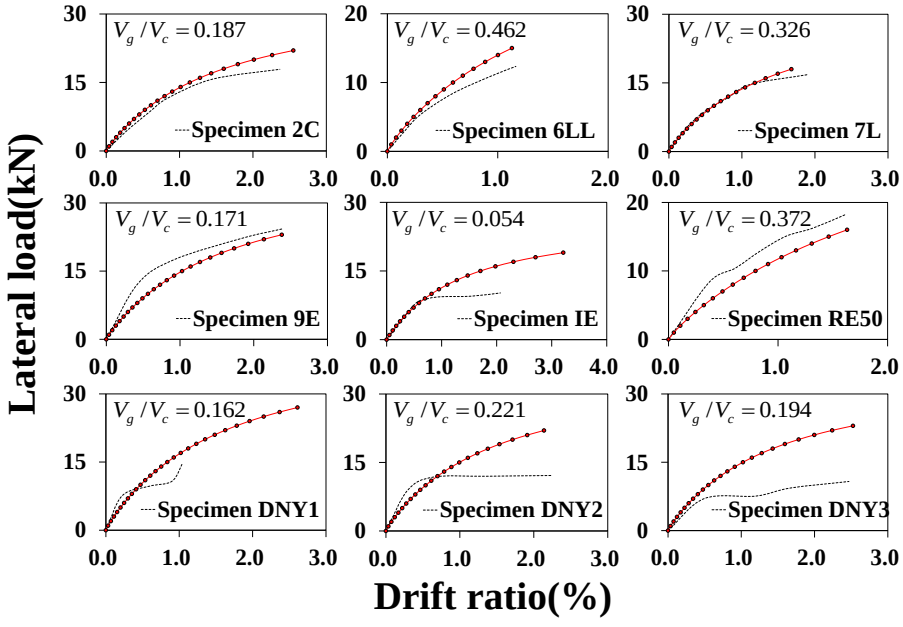

(b) Exterior slab-column connections

Fig. 7 Evaluation of the proposed model comparing to test results of slab-column connections

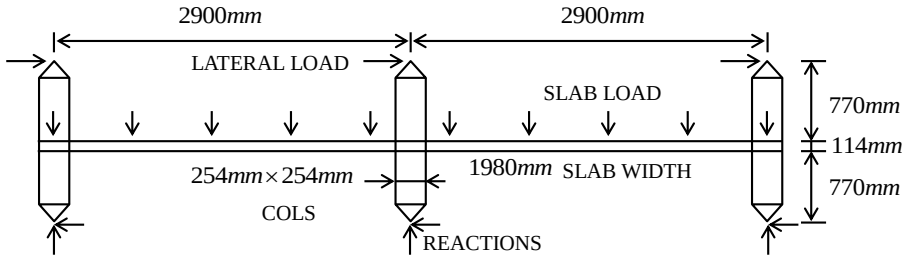

(a) test specimen (Robertson 1990, 1997)

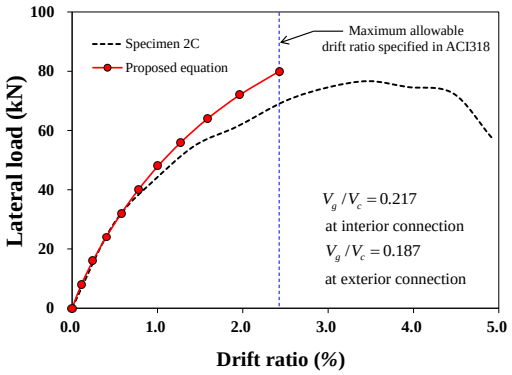

(b) specimen 2C

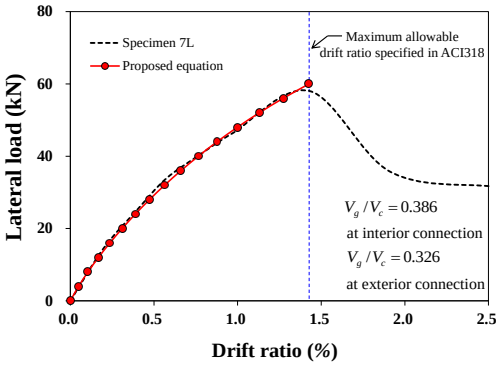

(c) specimen 7L

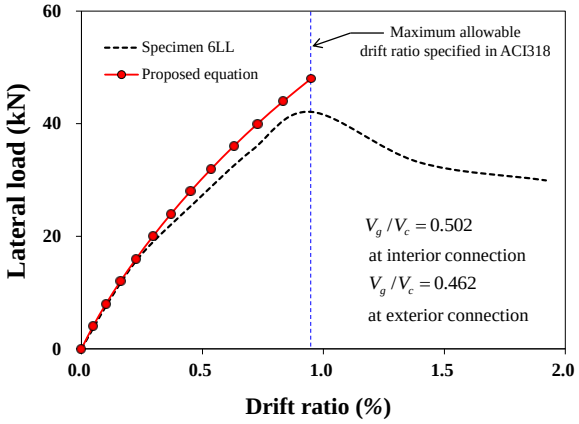

(d) specimen 6LL

Fig. 8 Verification of the proposed model comparing to test results of flat plate systems

5. Conclusion

In this paper, the unified equivalent frame method proposed in the companion paper was verified by using the UCB tests on the multi-span flat plate structure. Also, the stiffness reduction factors were derived for the exterior and interior slab-column connections, which were utilized to evaluate the nonlinear behavior of flat plate systems. On this basis, the following conclusions were drawn:

- The proposed UEFM, utilizing the combined application of the equivalent column and equivalent slab concepts, provided the accurate and rational estimations on the lateral responses of multi-span flat plate structures subjected to the combined gravity and lateral forces.
- In order to simulate the stiffness degradation of flat plate systems, this study proposed the stiffness reduction factors of the torsional member in the equivalent frame, which well captured the nonlinear lateral behavior of the flat plate systems in a simple way.
- The stiffness degradation of flat plate system after cracking can be appropriately estimated by applying the well-defined stiffness reduction factor to the torsional member, and it is appeared to be a simple way to reflect the nonlinear behaviour of flat plate.
- The displacement of the flat plate system at the maximum lateral loads was assessed by the method specified in ACI 318-11, which was simple but provided reasonably good analysis results.
- Further research on an advanced stiffness reduction factor is still required to estimate the post-peak response of flat plate systems. Additional research on the limit criteria for determination of deformation capacity of flat plate structures can also enhance the accuracy of UEFM proposed in this study.

Acknowledgment

The research was supported by the Basic Science Research Program through the National Research Foundation of Korea (NRF) funded by the Ministry of Education, Science and Technology (NRF-2013R1A1A2059504)

References

ACI Committee 318 (2011), Building Code Requirements for Structural Concrete and Commentary (ACI 318M-11), American Concrete Institute, Farmington Hills, 503.

Banchik, C.A. (1987), "Effective beam width coefficients for equivalent frame analysis of flat-plate Structures", ME Thesis, University of California, Berkley, CA.

Cano, M.T. and Kilngner, R.E. (1987), "Comparison of analysis procedures for tow-way slabs", *ACI Struct. J.*, **85**(6), 597–608.

Carvalho, G., Bento, R. and Bhatt, C. (2013), "Nonlinear static and dynamic analyses of reinforced concrete buildings – comparison of different modelling approaches", *Earthq. Struct.*, **4**(5), 451-470

Carr, A.J. (2005), RUAUMOKO—Inelastic Dynamic Analysis Program, Department of Civil Engineering, University of Canterbury, Christchurch, New Zealand.

Choi, K.K. and Park, H.G. (2003), "Moment-Rotation Relationship and Effective Stiffness of Flat Plates under Lateral Load", *J. Korean Concrete Inst.*, **15**(6), 856-865.

Corely, W.G., Sozen, M.A. and Siess, C.P. (1961), "The equivalent frame analysis for reinforced concrete slabs", Structural Research Series No. 218, Department of Civil Engineering, University of Illinois, Urbana, IL.

Corley, W.G. and Jirsa, J.O. (1970), "Equivalent frame analysis for slab design", *ACI J., Proc.*, **67**(11), 875-884.

Coronelli, D. (2010), "Grid model for flat-slab structures", *ACI Struct. J.*, **107**(6), 645-653.

Coronelli, D. and Corti, G. (2014), "Nonlinear static analysis of flat slab floors with grid model (with Appendix)", *ACI Struct. J.*, **111**(2), 343-352.

Du, Y. (1993), "Seismic resistance of slab-column connection in existing non-ductile flat-plate buildings", PhD. thesis, Rice University, Houston, TX.

Elnashai, A.S., Papanikolaou, V. and Lee, D. (2010), Zeus-NL - A System for Inelastic Analysis of Structures – User Manual, Mid-America Earthquake Center, Univ. of Illinois at Urbana-Champaign, Urbana, IL.

Ghobarah, A. (2001), "Performance-based design in earthquake engineering: State development", *Eng. Struct.*, **23**(8), 878-884.

Grossman, J.S. (1997), "Verification of proposed design methodologies for effective width of slabs in slab–column frames", *ACI Struct. J.*, **94**(2), 181-196.

Han, S.W., Park, Y.M. and Kee, S.H. (2009), "Stiffness reduction factor for flat slab structures under lateral loads", *J. Struct. Eng. - ASCE*, **135**(6), 743-750.

Hwang, S.J. and Moehle, J.P. (1993). "An experimental study of flat-plate structures under vertical and lateral loads", University of California, Berkeley, CA.

Hwang, S.J. and Moehle, J.P. (2000), "Models for laterally loaded slab–column frames", *ACI Struct. J.*, **97**(2), 345–352.

Karimiyan, S., Moghadam, A.S. and Vetr, M.G. (2013), "Seismic progressive collapse assessment of 3-story RC moment resisting buildings with different levels of eEccentricity in plan", *Earthq. Struct.*, **5**(3), 277-296

Kim, K.S., Choi, S.H., Ju, H.J., Lee, D.H., Lee, J.Y. and Shin, M.S. (2014), "Unified equivalent frame method for flat plate slab structures under combined gravity and lateral loads – Part 1: derivation", **7**(5).

Lee, S.J., Lee, D.H., Kim, K.S., Oh, J.Y., Park, M.K. and Yang, I.S. (2013), "Seismic performances of RC columns reinforced with screw ribbed reinforcements connected by mechanical splice", *Comput. Concrete.*, **12**(2), 131-149.

Luo, Y.H. and Durrani, A.J. (1995a), "Equivalent beam model for flat slab buildings – part I: Interior connection", *ACI Struct. J.*, **92**(1), 115–124.

Luo, Y.H. and Durrani, A.J. (1995b), "Equivalent beam model for flat slab buildings – Part II: Exterior connection", *ACI Struct. J.*, **92**(2), 250–257.

McKenna, F., Fenves, G.L., Scott, M.H. (2000), *Open System for Earthquake Engineering Simulation*, University of California, Berkeley, CA, Available from: http://opensees.berkeley.edu.

Moehle, J.P. and Diebold, J.W. (1985), "Lateral load response of flat-plate frame", *J. Struct. Eng. - ASCE*, **111**(10), 2149-2164.

Murray, K.A., Cleland, D.J., Gilbert, S.G. and Scott, R.H. (2003), "Improved Equivalent Frame Method for Flat Plate Structures in Vicinity of Edge Column", *ACI Struct. J.*, **100**(4), 454-464.

Pan, A. and Moehle, J.P. (1988), "*Reinforced Concrete Flat Plates under Lateral Load: An Experimental Study Including Biaxial Effects*", Report No. UCB/EERC-88/16, Earthquake Engineering Research Center, University of California, Berkeley, CA.

Park, Y.M., Han, S.W. and Kee, S.H. (2009), "A modified equivalent frame method for lateral load analysis", *Mag. Concrete Res.*, **61**(5), 359-370.

Prakash, V., Powell, G.H. and Campbell, S. (1993), DRAIN-2DX Base Program Description and User Guide: Version 1.10. SEMM *Report* No. 93/17, University of California at Berkeley, CA.

Robertson, I.N. (1990), "Seismic response of connections in indeterminate flat-slab subassemblies", Ph.D. thesis, Department of Civil Engineering, Rice University, Houston, TX.

Robertson, I.N. (1997), "Analysis of flat slab structures subjected to combined lateral and Gravity Loads", *ACI Struct. J.*, **94**(6), 723-729

Robertson, I.N., Kawai, T., Lee, J. and Enomoto, B. (2002), "Cyclic testing of slab-column connections with shear reinforcement", *ACI Struct. J.*, **99**(5), 605-613.

Robertson, I.N. and Johnson, G. (2006), "Cyclic lateral loading of non-ductile slab-column connections", *ACI Struct. J.*, **103**(3), 356-364.

Schwaighofer, J. and Collins, M.P. (1977), "Experimental study of the behavior of reinforced concrete coupling slabs", *ACI J., Proc.*, **74**(3), 123-127.

Vanderbilt, M.D. (1981), *The Equivalent Frame Analysis for Reinforced Concrete Slabs*, Structural Research Series No. 36, Civil Engineering Department, Colorado State University, Fort Collins, CO.
Vanderbilt, M.D. and Corley, W.G. (1983), "Frame analysis for concrete buildings", *Concrete Int.: Des. Construct.*, **5**(12), 33-43.

Notations

A_{cp} = sectional area of shear flow zone
c_1 = width of column in loading direction
c_2 = width of column in perpendicular to loading direction
d_{ave} = average effective depth of slab
C = torsional constant
E_c = modulus of elasticity of concrete
$f_c^{'}$ = specified compressive strength of concrete
K_c = flexural stiffness of column
K_{ec} = stiffness of equivalent column
K_{es} = stiffness of equivalent slab
K_s = flexural stiffness of slab-beam
K_I = actual stiffness of slab considering gravity shear effect
K_o = initial stiffness of slab without gravity shear effect
$K_{s,eff}$ = effective flexural stiffness of slab-beam considering gravity shear effect
K_{t,λ_c} = effective stiffness of torsional member in flat plate system subjected to gravity and lateral load
L_1 = slab width of the design strip
L_2 = slab width perpendicular to the design strip
M_{ub} = unbalance moment due to lateral load
p_{cp} = perimeter of shear flow zone
t = thickness of slab
T_{cr} = cracking strength of attached torsional member
V_g = external gravity shear force
V_c = punching shear strength in 2-way slab
η_l = initial stiffness reduction factor due to gravity shear
$\eta_{l,\text{ext}}$ = stiffness reduction factor of attached torsional member due to lateral load in exterior connection
$\eta_{l,\text{int}}$ = stiffness reduction factor of attached torsional member due to lateral load in interior connection
λ_c = load ratio factor
χ = slab stiffness reduction factor
$\theta_{gravity}$ = rotational contribution of torsional member to equivalent column
$\theta_{lateral}$ = rotational contribution of torsional member to equivalent slab
h_1 = height of upper column
h_2 = height of bottom column